Korean J. Chem. Eng., 36(3), 345-355 (2019)
DOI: 10.1007/s11814-018-0210-x

pISSN: 0256-1115
eISSN: 1975-7220

Techno-economic optimization of the integration of an organic Rankine cycle into a molten carbonate fuel cell power plant

Kyungtae Park*, Soung-Ryong Oh, and Wangyun Won***,†**

*Department of Chemical and Biological Engineering, Sookmyung Women's University, Seoul 04310, Korea
**R&D Center, Gas Technology Compression Company, Changwon, Gyeongnam 52032, Korea
***Department of Chemical Engineering, Changwon National University, Changwon, Gyeongnam 51140, Korea
(Received 23 August 2018 • accepted 13 December 2018)

Abstract−This study proposes a simple economic model to optimize the integration of an organic Rankine cycle into a molten carbonate fuel cell power plant. The optimization was conducted with five different types of working fluids, and an exergetic optimization was also done for comparison. In addition, sensitivity analysis was conducted to provide better insight into the behavior of the ORC system. The optimization results show that the optimum economic point and the optimum exergetic point are different, and a maximum profit can be achieved for the ORC system with economic optimization. Overall, in most cases, the profit is highest when the ORC system uses n-butane; however, R152a yields better profit when the ambient temperature is below 5 °C. In addition, all ORC systems show positive profit when the price of electricity is above 0.05 USD/kWh. For sensitivity analysis, two simulation experiments were conducted to observe the effect of changes in the feed gas temperature and the sales price of electricity on the optimization results. As a result, changes in the sale price of electricity are very critical, but changes in the feed gas temperature are not important.

Keywords: Techno-economic Optimization, Organic Rankine Cycle, Molten Carbonate Fuel Cell Power Plant, Particle Swarm Optimization, Simulation

INTRODUCTION

Currently, the development of efficient process for energy recovery from waste heat is a critical problem due to escalating energy prices and strict environmental regulations. Therefore, research efforts should focus on recovering energy from various waste heat sources including geothermal, solar, biomass, etc., in order to achieve more efficient energy use.

One interesting approach is to recover the energy required to produce electricity from the flue gas of a molten carbonate fuel cell (MCFC) power plant. Because MCFCs are highly efficient fuel cells that do not emit SO_x and NO_x [1], many small-scale fuel cell power plants employ MCFC all around the world [2,3]. MCFC power plants can improve their efficiency by combining MCFC fuel cells with heat recovery systems because they operate at temperatures above 600 °C, and the flue gases also have high temperatures.

There are many methods for the recovery of heat from waste gases, but the organic Rankine cycle (ORC) has attracted significant attention. Since a conventional Rankine cycle is not efficient for the recovery of low grade waste heat [4,5], ORC systems use various organic working fluids with lower boiling points than water. However, recovering energy from a waste heat source is always accompanied by cost and efficiency issues.

Therefore, many studies have investigated the performance of ORC systems from various perspectives. Akkaya and Sahin studied a solid oxide fuel cell that was integrated with an ORC (SOFC-ORC) system [6], and Anagelino et al. and Ji et al. investigated molten carbonate fuel cells combined with an ORC (MCFC-ORC) system [7,8]. Mamaghani et al. proposed an MCFC gas turbine with an ORC (MCFC-GT-ORC) system [9], and Ebrahimi and Moradpoor suggested an SOFC micro-gas turbine with an ORC (SOFC-MGT-ORC) system [10]. These studies have shown that ORCs can improve the efficiency of fuel cells by recovering energy from waste gases.

Other studies have focused on the selection of an ORC working fluid. Wang et al. determined that R245fa and R245ca had the best performance for the recovery of waste heat from the flue gas in a vehicle's engine [11]. Sánchez et al. proved that R245fa is the best working fluid in terms of thermal efficiency for an MCFC-GT-ORC system [12]. Desideri et al. experimentally compared SES36 and R245fa for waste heat recovery applications [13], and concluded that R245fa is better than SES36 in terms of electrical power output. Sun et al. investigated 400 combinations of working fluids for a two-stage ORC using LNG cold energy [14]; and Lee and Han proposed a multi-component ORC to recover LNG cold energy [15]. These studies have shown that the selection of an ORC working fluid has a significant effect on the performance of ORC and that the preferred working fluid depends on the intended application.

Other studies have tried to find optimal conditions and designs for ORC systems. Li et al. studied the effect of evaporation temperature on the thermal efficiency of the ORC system and compared the performance of a standard ORC system to an ORC system equipped with an internal heat exchanger [16]. Sarkar proposed a generalized pinch-point design strategy to optimize the operating

†To whom correspondence should be addressed.
E-mail: wwon@changwon.ac.kr

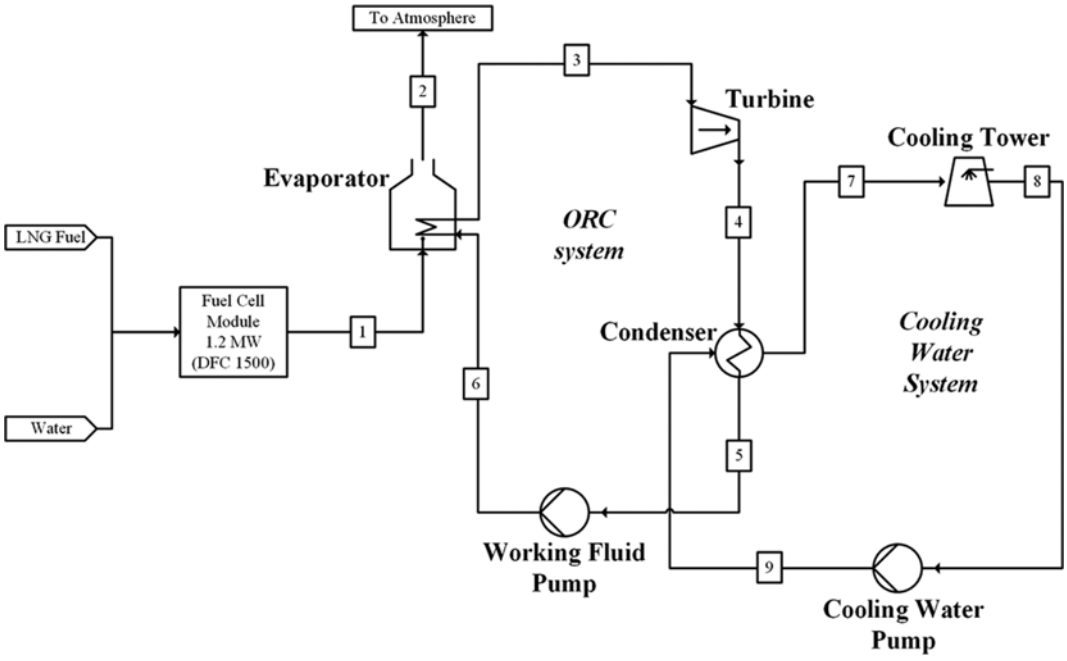

Fig. 1. Flow diagram of the overall process for a simple ORC system integrated into an MCFC power plant.

conditions of the ORC system [17] and found that the evaporation and condensation temperatures affected the performance of the ORC system. Wang et al. evaluated five different types of ORC systems and compared the performance of each system [18].

As mentioned, the effectiveness of an ORC system that has been integrated into a fuel-cell power plant, the importance of the working fluid and the optimization of these ORC systems have been well studied. However, economic analysis is essential in order to implement ORC systems for waste heat recovery. Most previous work has focused on the thermal or exergy efficiencies or electrical power output of ORC systems, but these factors do not guarantee economic optimization. Although several studies have addressed the economic model of ORC systems, they estimated the cost of the ORC system based on the capacity factor [19-21] or they did not optimize the ORC system in terms of the economy [22].

Therefore, in this study, a simple economic model to estimate the cost of an ORC system integrated into a 1.2 MW MCFC power plant is proposed and a techno-economical optimization was performed. The economic model to estimate the profit of the ORC system was developed using the concept of total annualized cost, and particle swarm optimization was used to find the optimal solution. A simulation model for ORC systems was also developed to perform techno-economic optimization using a commercial simulation software (ASPEN PLUS V10). For comparison, exergetic optimization was also performed. Finally, to investigate the effects of changes in key economic parameters, a sensitivity analysis was conducted.

BACKGROUND THEORY

1. The Organic Rankine Cycle (ORC)

An ORC system is a Rankine cycle that uses an organic working fluid with a lower boiling point than water to recover low temperature heat. Therefore, the main purpose of using an ORC system is produce electricity by recovering heat from low temperature heat sources such as geothermal energy, solar thermal energy, and waste heat from power plants to produce electricity.

The ORC system can be classified into several types, such as a simple ORC, an ORC with an internal heat exchanger, an ORC with an open feed organic fluid heater, an ORC with a closed feed organic fluid heater, and an ORC with a reheater [18]. Among them, a simple ORC system is adopted in this study, and the process flow diagram of a simple ORC system used in this study is shown in Fig. 1.

The simple ORC system generally consists of expanders, condensers, pumps, and evaporators. The working principle of the ORC is very similar to the original Rankine cycle. In the simple ORC system, working fluid is pumped to the evaporator (stream 6), heat from heat sources in the evaporator is recovered, and it is expanded by passing through the turbine (stream 3 to stream 4). In the turbine, part of the recovered heat is converted into useful work. Finally, the expanded working fluid is condensed by the condenser (stream 4 to stream 5).

The selection of a working fluid is very important because the working fluid has a significant effect on the overall performance of the ORC system. The working fluid can be categorized as 'wet', 'dry' or 'isentropic' based on the shape of the vapor saturation curve in the temperature-entropy (T-s) diagram. T-s diagrams for typical working fluids in ORC systems are shown in Fig. 2. Generally, dry and isentropic fluids are preferred over wet fluids because wet fluids require a high degree of superheating at the evaporator outlet in order to avoid two-phase conditions at the turbine outlet.

2. The Particle Swarm Optimization (PSO) Algorithm

The PSO algorithm is a population-based stochastic search

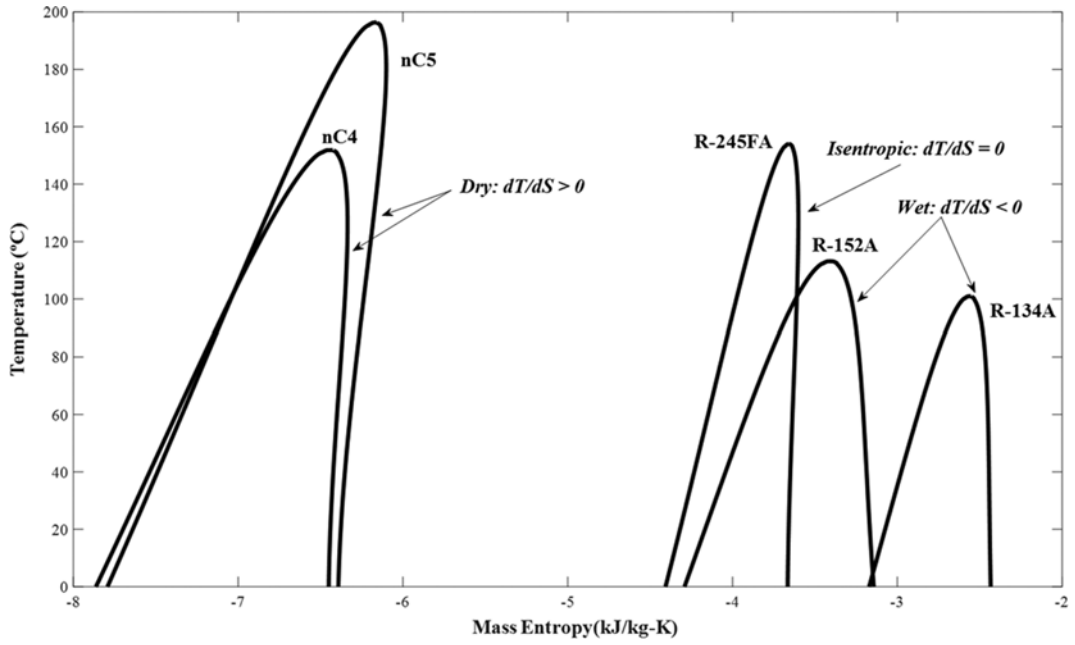

Fig. 2. T-s diagrams of typical working fluids in an ORC system.

method that has been applied to many complicated optimization problems. Compared to other swarm intelligence algorithms, the PSO algorithm is easy to implement, performs well and can be applied to many real world problems due to its simplicity [23-25]. Although the PSO algorithm cannot guarantee a globally optimized solution, may reports have shown that it can be used to find excellent near-optimal solutions [26-28].

The PSO algorithm generates a swarm of particles that fly throughput the searching space to find the global optimal solution. Each particle represents a candidate for the solution and is initialized to a random position and velocity. Each particle updates its position using the following equations:

$$v_j^{i+1} = w_j v_j^i + c_1 r_1 (pbest_j^i - x_j^i) + c_2 r_2 (gbest^i - x_j^i) \quad (1)$$
$$x_j^{i+1} = x_j^i + v_j^{i+1}$$

where v_j^i is the velocity vector of the *j*-th particle at the *i*-th iteration; w_j is the inertia weight at the ith iteration; c_1 is the self-adjustment weight that pulls the particles toward pbest; c_2 is the social-adjustment weight that pulls the particles toward gbest; r_1 and r_2 are random numbers uniformly distributed between [0, 1]; $pbest_j^i$ is the best position found by the j-th particle until the i-th iteration; $gbest^i$ is the best position found by the entire swarm until the i-th iteration; and x_j^i is the position of the j-th particle at the i-th iteration. In addition to Eq. (1), a detailed PSO algorithm is illustrated in Fig. 3.

SIMULATION MODEL AND MATHEMATICAL FORMULATION

1. Description of the Target ORC System

In this study, the target ORC system is the one integrated into an MCFC power plant in order to recover heat from flue gas and

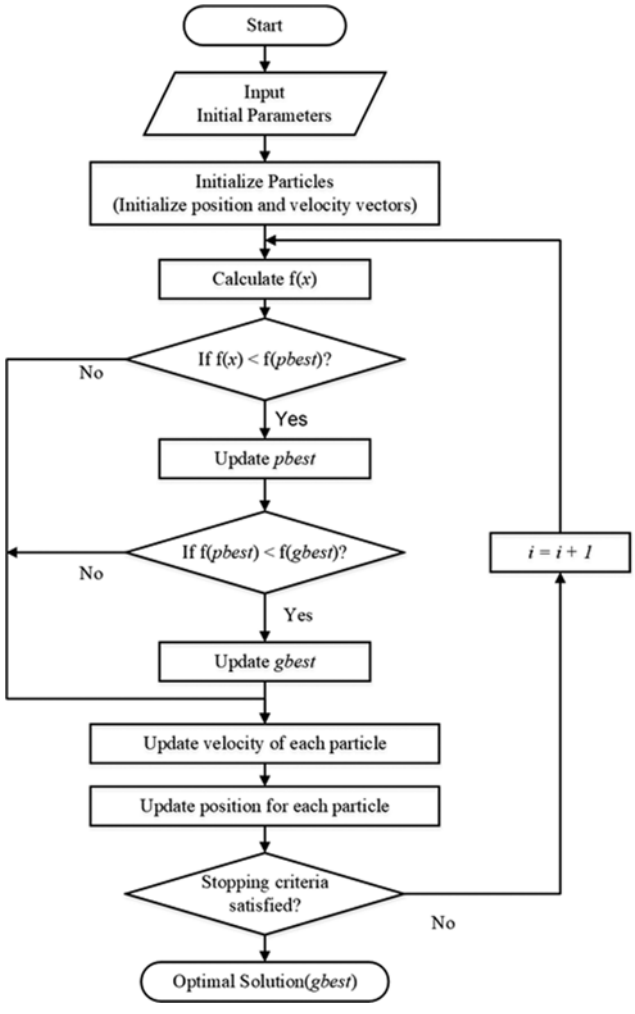

Fig. 3. A detailed PSO algorithm.

Table 1. The feed gas conditions of the ORC system

Stream No.		1	2
Temperature (°C)		390	100
Pressure (bar)		1.026	1.020
Flowrate (kg/h)		7300	7300
Composition (mol %)	CO_2	4.5	4.5
	O_2	9.5	9.5
	H_2O	19.5	19.5
	N_2	66.5	66.5

Table 2. Details of the developed simulation model

Input parameters	Values
Property package	Peng-Robinson
Pump efficiency (%)	57
Turbine efficiency (%)	72
Evaporator pressure drop (Hot/Cold) (bar)	0.006/0.2
Condenser pressure drop (Hot/Cold) (bar)	0.2/0.2
Cooling tower outlet pressure (bar)	1.013
Cooling water pump outlet pressure (bar)	3
Ambient temperature (°C)	15
Decision variables	**Initial values**
Working fluid mass flow rate, m_6 (kg/hr)	11000
Turbine outlet pressure, P_4 (bar)	2.8
Working fluid pump outlet pressure, P_6 (bar)	17
Condenser outlet temperature, T_5 (°C)	68
Simulation results used for optimization	**Notation**
Electricity generated by turbine (kW)	W_t
Electricity consumed by pumps (kW)	W_p
Heat exchange area values of heat exchangers (m^2)	A
Cooling water volumetric flow rate (m^3)	V_{cw}

generate the electricity. The overall process flow diagram of the ORC system integrated into a 1.2 MW MCFC power plant are shown in Fig. 1; the feed gas (the flue gas from the fuel cell module) conditions [7,29] are summarized in Table 1, and details of the developed simulation model are summarized in Table 2.

As shown in Table 2, the mass flowrate of the working fluid (m_6), the turbine outlet pressure (P_4), the condenser outlet temperature (T_5), and the working fluid pump outlet pressure (P_6) were selected as the decision variables for performing the optimization according to the results of the degrees of freedom analysis. In addition, R134a, R152a, R245fa, n-butane and n-pentane were selected as the working fluids for the target ORC system based on previous studies [7,30,31].

2. Mathematical Formulation

The objective function of the ORC system optimization problem is established as follows:

$$f=\text{Profit}=\text{Revenue}-\text{Expenditures} \tag{2}$$

The following assumptions were used to formulate the optimization problem:

1) The only revenue source for the ORC system is assumed to be the electricity generated from the turbine, and the produced electricity is connected to the power grid and sold.

2) To simplify the problem, the concept of total annualized cost (TAC) [32,33] was applied to estimate Expenditures.

3) Only the purchase and installation costs of the main equipment were considered as capital costs.

4) Only the cost of electricity was considered as an operational cost.

Based on the assumptions mentioned above, the Revenue in Eq. (2) can be calculated by the following equation:

$$\text{Revenue}=W_t * P_{elec} * t_{oper} \tag{3}$$

As mentioned, the concept of TAC is applied to estimate the Expenditures in Eq. (2). Therefore, Expenditures can be expressed as follows [34,35]:

$$\text{Expenditures}=J_{operation}+J_{capital} \tag{4}$$

$$J_{operation}=\sum_p W_p * P_{elec} * t_{oper} \tag{5}$$

$$J_{capital}=\sum_q PC_q/t_{depr} \tag{6}$$

where $p\in$ {cooling water pump, working fluid pump}; and $q\in$ {evaporator, turbine, condenser, working fluid pump, cooling tower, cooling water pump}. The annualized operation cost ($J_{operation}$) was estimated by adding the annual electricity cost of the cooling water pump and the working fluid pump, and the annualized capital cost ($J_{capital}$) was estimated by adding a depreciation cost of all equipment in the ORC system.

PC_q was estimated based on previous research data [36] and adjusted to USD in 2017 using the chemical engineering plant cost index (CEPCI) [37] because the previous research data were estimated in 1998. The PC_q of each piece of equipment, q, can be calculated by the following equations:

$$PC_{evap}=37940 * A^{0.5155} * \frac{CI_{2017}}{CI_{1998}} \tag{7}$$

$$PC_{cond}=(198.36 * A+52635) * \frac{CI_{2017}}{CI_{1998}} \tag{8}$$

$$PC_{cwtower}=(112.23 * V_{cw}+56221) * \frac{CI_{2017}}{CI_{1998}} \tag{9}$$

$$PC_{turbine}=(-0.17 * W_t^2+309.13 * W_t+33516) * \frac{CI_{2017}}{CI_{1998}} \tag{10}$$

$$PC_{wfpump}=(11974 * W_{wfpump}^{0.502}) * \frac{CI_{2017}}{CI_{1998}} \tag{11}$$

$$PC_{cwpump}=(52.02 * V_{cw}+22746) * \frac{CI_{2017}}{CI_{1998}} \tag{12}$$

where CI_{1998} and CI_{2017} stand for the CEPCIs in 1998 and 2017, respectively. Please note that a reciprocating working fluid pump and centrifugal cooling water pump are assumed.

Finally, the optimization problem can be defined as follows:

$$\max.f(x)=\min.-\left(W_t * P_{elec} * t_{oper} - \left(\sum_p W_p * P_{elec} * t_{oper}+\sum_p PC_q/t_{depr}\right)\right) \tag{13}$$

subject to

$$P_5^{sat} + \Delta P_{cond} \le P_4 \le P_3 \quad (14)$$

$$T_3 < T_c \quad (15)$$

$$T_9 + 5 \le T_5 \le T_4 \quad (16)$$

$$vf_3,\ vf_4 = 1 \text{ and } vf_5 = 0 \quad (17)$$

$$P_5 \le P_6 \le P_c \quad (18)$$

$$3000 < m_6 \le 20000 \quad (19)$$

$$T_8 = T_{AMB} + 5 \quad (20)$$

$$T_7 = T_9 + 5 \quad (21)$$

where x is a set of the decision variables, $x \in \{P_4, T_5, P_6, m_6\}$. Eqs. (14) to (21) are the process constraints used to obtain realistic optimization results. For instance, Eq. (14) prevents cavitation in the pump by preventing the pump inlet pressure (P_5) from falling below the saturation pressure (P_5^{sat}); Eqs. (15) and (18) prevent the ORC system from operating in supercritical conditions as preventing the highest pressure (P_3) and the highest temperature (T_3) of the ORC system from exceeding the critical condition of a working fluid; To ensure a practical heat exchange area, the temperature difference between the hot and cold fluids of a heat exchanger was assumed as 5 °C in this study and Eqs. (16), (20) and (21) represent it; Eq. (17) protects the turbine and the working fluid pump from damage caused by liquid droplets or vapors.

Exergetic analysis is a part of thermodynamic analysis based on the second law of thermodynamics. The exergy efficiency can be calculated [16,30] as follows:

$$\psi_{ORC} = \frac{W_{net}}{Q_{IN}\left(1 - \frac{T_{AMB}}{T_{evap}}\right)} \quad (22)$$

$$W_{net} = W_{turbine} - \sum_p W_p \quad (23)$$

Therefore, the objective function to maximize the exergy efficiency can be defined as follows:

$$\max. \psi_{ORC} = \min. - \frac{W_{net}}{Q_{IN}\left(1 - \frac{T_{AMB}}{T_{evap}}\right)} \quad (24)$$

subject to Eqs. from (14) to (21).

The proposed optimization model is formulated as a non-linear problem mainly due to the non-linearity between the decision variables (P_4, T_5, P_6, m_6) and the generated electricity (W_t and W_p). In addition, the purchase cost (PC_q) and some process variables have a non-linear relationship in this problem as shown in Eqs. (7)-(12). To solve the optimization problem, the ORC system simulation model created by ASPEN PLUS V10 was integrated with MATLAB using a component object model (COM) interface [38], and the optimal solution was found using the PSO algorithm in MATLAB.

OPTIMIZATION RESULTS

This section describes the optimization results for the ORC system. The results from the base case will be described first, followed by the results from the sensitivity analysis.

Table 3. Set algorithm values and parameters for the base case

	Items	Values
PSO settings	Self-adjustment weight (c_1)	0.99
	Social-adjustment weight (c_2)	1.99
	Max. iteration number	100
	Number of particles	40
Parameters	Electricity sales price (P_{elec}) [39]	0.07 USD/kWh
	Capital depreciation time (t_{depr})	20 years
	Operation hours (t_{oper})	8059.2 hours
	CEPCI (CI_{2017}, CI_{1998}) [40]	CI_{2017}=672
		CI_{1998}=436

1. Base Case

The set values for the PSO algorithm and key parameters for the base case are summarized in Table 3.

To confirm the performance of the PSO algorithm, performance comparison between the PSO algorithm, the genetic algorithm (GA), the simulated annealing (SA) algorithm, and the pattern search (PS) algorithm was performed for the base case. As a result, the PSO algorithm has the best performance among them, and the results are summarized in Fig. 4.

As shown in Fig. 4, the PSO algorithm shows the best performance with the lowest objective function value (–9190.2 USD/year). The GA and the SA also found the objective function values, but these values are higher than the value of the PSO algorithm. The PS algorithm did not find the solution.

In addition, several simulation experiments for the base case were performed with various initial conditions to ensure the stability of the solution obtained by the PSO algorithm. As a result, the same objective function values were obtained regardless of the initial conditions. The results are summarized in Table 4.

Optimization results for the base case are summarized in Table 5. As shown in Table 5, the ORC system uses n-butane has the maximum Profit when the Profit objective function was maximized. The results clearly indicate that the exergetic optimization does not guarantee an economic optimum. The economic optimum point of the ORC system was found when the Profit objective function was maximized, but this is not the optimum point in terms of exergy efficiency. The exergetic optimum of the ORC system was found when ψ_{ORC} was maximized, but the Profit of this case is much lower than that of the economic optimum point.

The Profit is lower in the max. ψ_{ORC} case than in the max. Profit case due to the high capital cost of the condenser (see Fig. 5). For the max. ψ_{ORC} case, the capital cost of the condenser accounts for about 19% of the Expenditures, whereas for the max. Profit case, the capital cost of the condenser accounts for about 15% of the Expenditures. As shown in Fig. 6, exergetic optimization tends to reduce the loss of exergy in the condenser by reducing the minimum internal temperature. However, this results in a high heat exchanger area and a high capital cost of the condenser.

In addition, the tested dry and isentropic fluids tend to perform better than the wet fluids in terms of Profit because of their low Expenditures. Key process variables and a detailed breakdown of

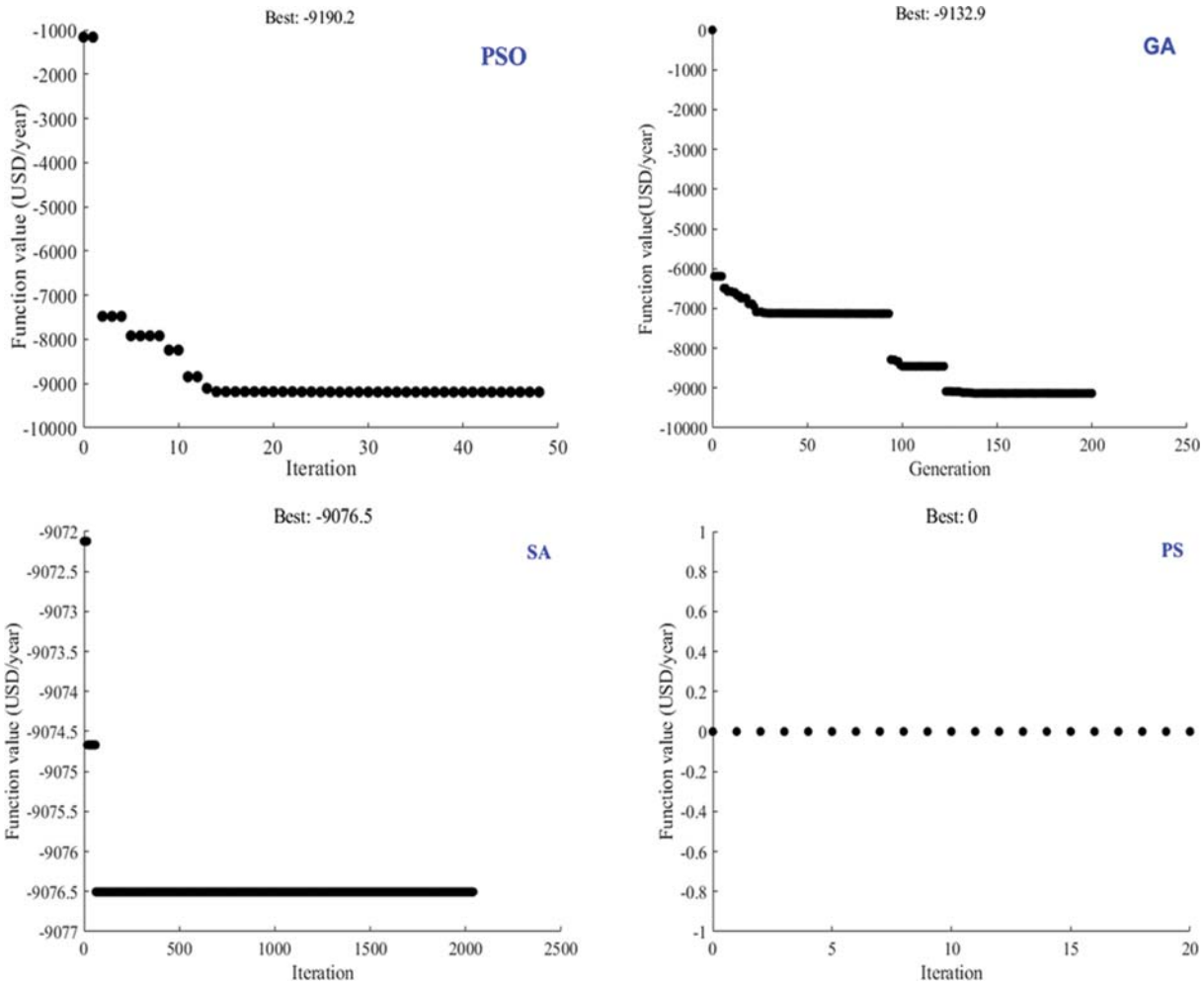

Fig. 4. Performance comparison results between optimization algorithms for the base case when the working fluid is n-butane.

Table 4. Results of simulation experiments for testing stability of the PSO algorithm

Case No.	Initial conditions				Objective function value (USD/year)
	Working fluid pump outlet pressure (P_6, bar)	Condenser outlet temp. (T_5, °C)	Turbine outlet pressure (P_4, bar)	Working fluid flowrate (m_6, kg/hr)	
1	17	68	2.8	11000	9190.2
2	17	235	2.8	5000	9190.2
3	10	243	4.9	8000	9190.2
4	25	59	17.4	14000	9190.2

Table 5. Optimization results for the base case

	max. Profit		max. ψ_{ORC}	
	Profit (USD/year)	ψ_{ORC} (%)	Profit (USD/year)	ψ_{ORC} (%)
R134a	−1,037	42.02	−2,438	44.45
R152a	5,355	46.79	2,859	48.33
R245fa	6,220	41.68	4,174	46.86
n-Butane	9,190	43.80	6,780	48.60
n-Pentane	7,379	39.44	7,378	39.44

the Expenditures for the max. Profit case are given in Tables 6 and 7. As shown in Tables 6 and 7, wet fluids have high operational and capital costs for the working fluid pump because the operating pressures of wet fluids are higher than those of dry or isentropic fluids to avoid two-phase conditions at the turbine outlet.

2. Sensitivity Analysis

To perform the sensitivity analysis, T_{AMB}, P_{elec} and T_1 were selected as the varying variables.

1) Changes in the ambient temperature (T_{AMB})

Changes in the ambient temperature lead to changes in the con-

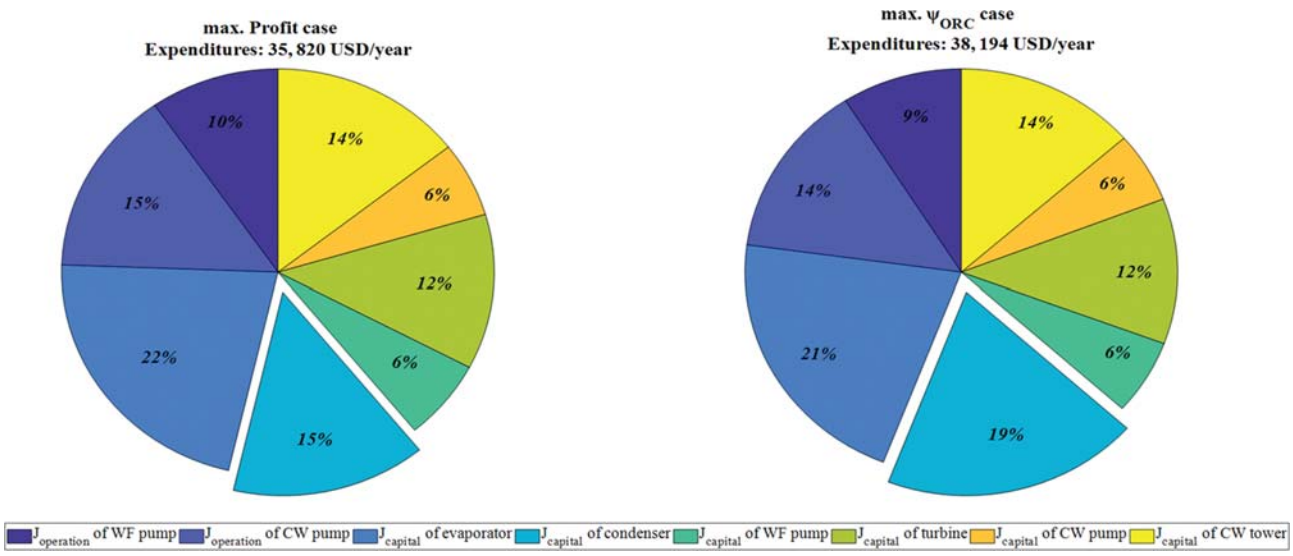

Fig. 5. A detailed breakdown of the Expenditures when the working fluid is n-butane.

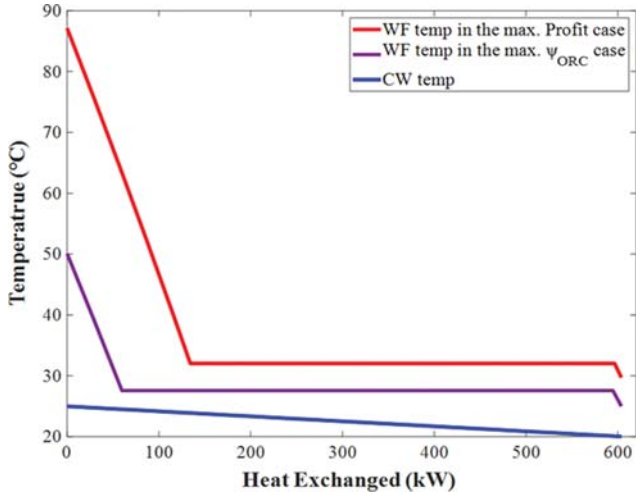

Fig. 6. T-Q diagram of the condenser when the working fluid is n-butane (Duty=603.8 kW).

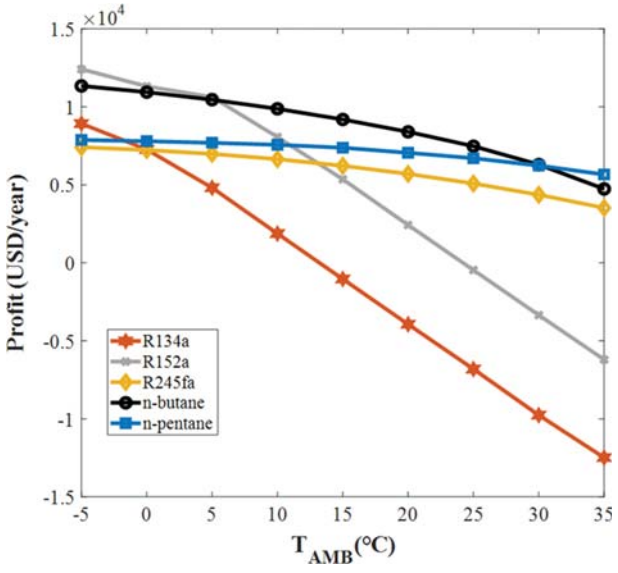

Fig. 7. The results of the sensitivity analysis with changes in the ambient temperature.

densation temperature (T_5) according to Eqs. (16) and (20). Therefore, simulations were conducted to determine the effect of ambient temperature changes on the performance of the ORC system. The ambient temperature was varied from −5 °C to 35 °C in 5 °C intervals, and all other variables and parameters remained the same as those used in the base case.

The results of this sensitivity analysis are shown in Fig. 7, and the ORC system using n-butane is most profitable when T_{AMB} is between 5 °C (not included) and 30 °C. On the other hand, the ORC system using R152a is most profitable when T_{AMB} is between −5 °C and 5 °C, and n-pentane is most profitable when T_{AMB} is over 30 °C. Interestingly, R134a and R152a tend to significantly increase the Profit as T_{AMB} decreases because they have lower boiling temperatures than other working fluids.

Fig. 8 illustrates the T-s diagrams of R152a (top) and n-butane

Table 6. Key process variables for the max. Profit case

	R134a	R152a	R245fa	n-Butane	n-Pentane
Electricity production (kW)	71.63	80.63	70.67	79.78	70.70
Electricity consumed (kW)	21.82	20.20	13.49	15.52	12.17
Net electricity production (kW)	49.81	60.43	57.18	64.26	58.53
Evaporator inlet pressure (bar)	32.7	33.1	12.9	18.2	7.5

Table 7. A detailed breakdown of the Expenditures for the max. Profit case

	Items	R134a	R152a	R245fa	n-Butane	n-Pentane
$J_{operation}$ (USD/year)	Working fluid pump	6891	6073	2246	3461	1516
	Cooling water pump	5421	5321	5363	5292	5351
	Sum	12312	11394	7608	8753	6867
$J_{capital}$ (USD/year)	Evaporator	7864	7398	7656	7842	7893
	Condenser	6462	6558	5004	5216	4702
	Turbine	4224	4421	4203	4403	4204
	Working fluid pump	3241	3042	1846	2294	1516
	Cooling water pump	2151	2143	2147	2141	2146
	Cooling tower	5191	5175	5182	5171	5180
	Sum	29133	28738	26037	27066	25640

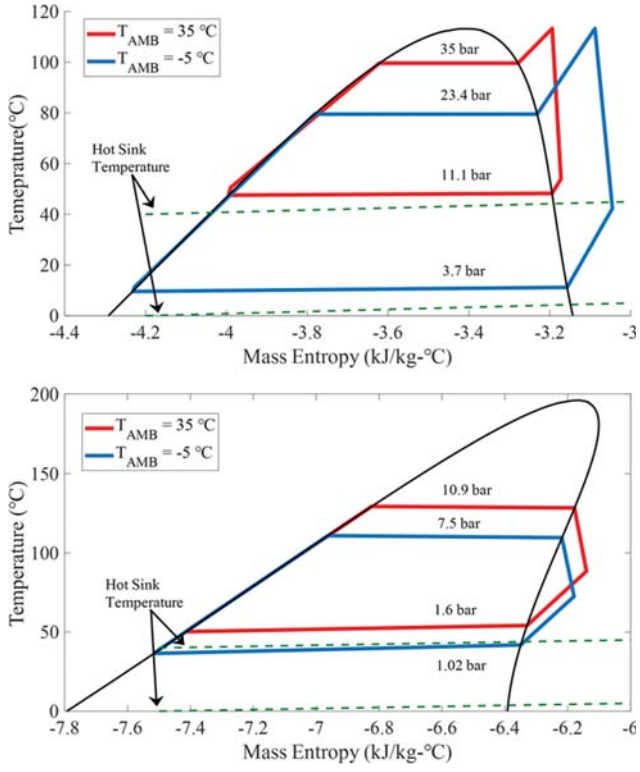

Fig. 8. The T-s diagrams of R152a (top) and n-butane (bottom).

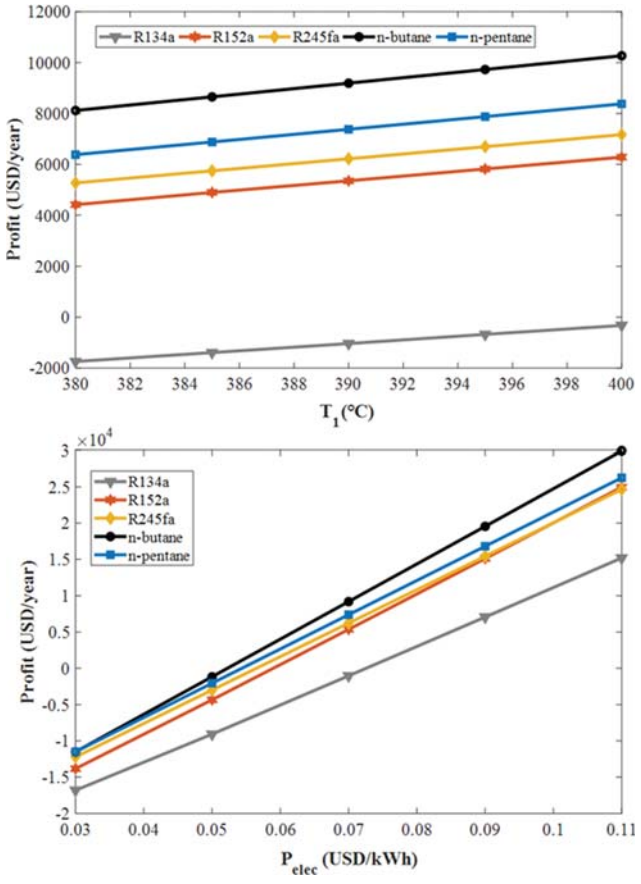

Fig. 9. The results of the sensitivity analyses with changes in the flue gas temperature (top) and changes in the electricity sales price (bottom).

(bottom). As shown in Fig. 8, the T-s diagram of R152a shrinks in area significantly as T_{AMB} value decreases. This suggests that the ORC system can generate more work because the area surrounded by the blue line is much larger than the area surrounded by the red line.

On the other hand, the T-s diagram of n-butane does not significantly improve the performance of the ORC system because it only slightly shrinks as the T_{AMB} value decreases. These two working fluids exhibit different behaviors because they have different boiling points. For example, the boiling point of R152a is −25 °C (at 1.013 bar) and that of n-pentane is 36.1 °C (at 1.013 bar). Therefore, to reach the saturated liquid state at high T_{AMB}, R152a requires high pressure, while n-pentane requires relatively low pressure. However, at low T_{AMB}, R152a has the potential to generate more work by lowering the condensation pressure as T_{AMB} value decreases, while n-pentane does not.

2) Changes in the flue gas temperature (T_1) and sales price of electricity (P_{elec})

Changes in the flue gas temperature lead to changes in the amount of work exchanged in the ORC system, and changes in the sales price of electricity lead to changes in the Revenue. Therefore, two simulation experiments were conducted to determine the effects

of changes in the flue gas temperature and the sales price of electricity changes on the performance of the ORC system. The first experiment varied the flue gas temperature from 380 °C to 400 °C at 5 °C intervals. The second experiment varied the electricity sales price from 0.03 USD to 0.11 USD at 0.20 USD intervals, and all other variables and parameters remained the same as those used in the base case.

The results are given in Fig. 9 where, as shown, the Profit linearly increased as T_1 and P_{elec} increase. When P_{elec} is less than 0.05 USD/kWh, all ORC systems have a negative Profit regardless of the working fluid. Notably, the slope of the Profit line for each working fluid is different in relation to the changes in the P_{elec}. The working fluid that can generate more electricity tends to be more profitable as P_{elec} increases, while the working fluid that requires lower Expenditures tends to be more profitable as P_{elec} decreases. For instance, the ORC system using n-pentane is more profitable than the ORC system using n-butane at P_{elec}=0.03 USD/kWh due to lower Expenditures, while the ORC system using R152a is more profitable than the ORC system using R245fa at P_{elec}=0.11 USD/kWh due to high electricity production.

Fig. 10 shows the tornado chart for the ORC system, where a change in P_{elec} has the greatest impact on the Profit, while the change in T_1 has the least impact. Overall, the performance of the ORC system using n-butane is best, but the ORC system using R152a is better at low ambient temperatures.

CONCLUSIONS

A techno-economic analysis was conducted on an ORC system integrated into a 1.2 MW MCFC power plant. A simulation model was developed using the commercial software ASPEN PLUS V10, a mathematical model was developed for economic optimization, and the concept of total annualized cost was applied to the mathematical model to simplify the problem. An exergetic optimization was also performed for comparison.

In the max. Profit case, the economic optimum point of the ORC system was found when the ORC system used n-butane. For the max. ψ_{ORC} case, the exergetic optimum point of the ORC system was found; however, the Profit was much lower than the economic optimum point due to the high heat exchange area of the condenser.

Overall, the ORC system using n-butane showed the greatest profit in most cases. However, the ORC system using R152a performed better at low ambient temperatures (below 5 °C in this study). This is quite an interesting result because, generally, wet fluids are not preferred over dry or isentropic fluids in ORC systems because they require a high degree of superheating, as mentioned in section 2.1. However, the results of this study show that some wet fluids can perform better than dry and isentropic fluids at low ambient temperatures due to their low boiling points.

According to the sensitivity analysis, changes in the feed gas temperature do not have a significant effect on the performance of the ORC system, but changes in the sales price of electricity are very critical. Notably, all ORC systems have positive profits when the sales price of electricity is above 0.05 USD/kWh.

The results of this study show that integrating an ORC system into a 1.2 MW MCFC power plant can generate profit, and optimization should be done from an economic point of view. In addition, the selection of a working fluid is very important, as fluid should be selected by considering the ambient temperature and sales prices of electricity. In future work, a life-cycle cost analysis of ORC system that considers ozone depletion potentials, global warming poten-

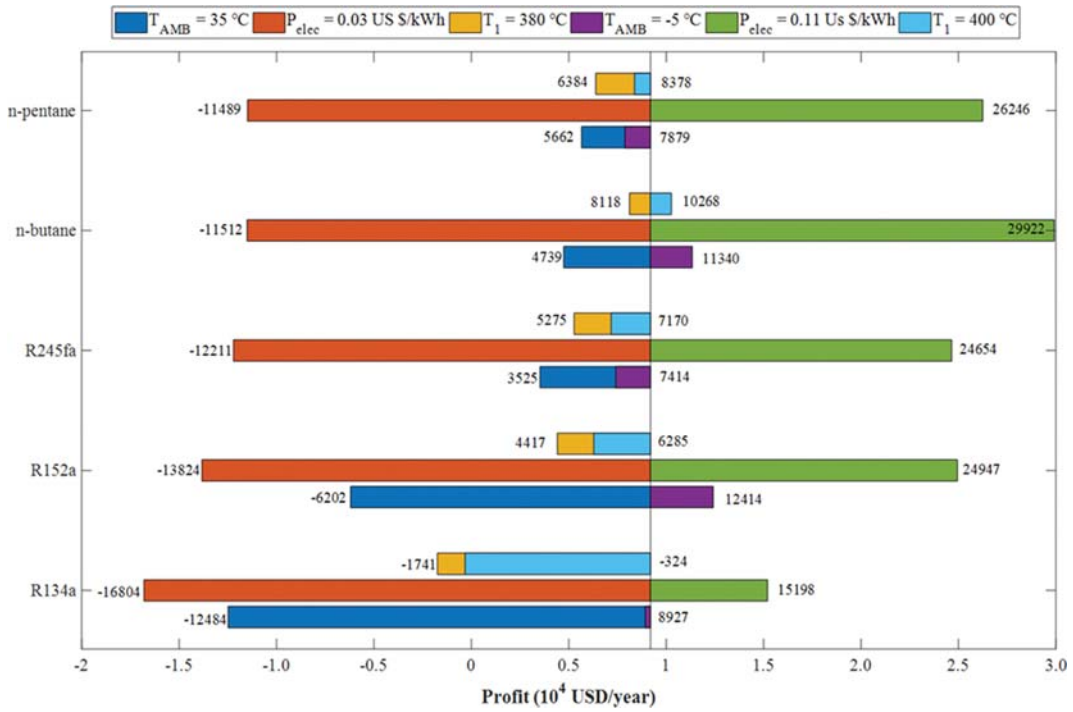

Fig. 10. Tornado chart of the ORC system.

tials and explosion risk will be conducted in order to obtain a more comprehensive techno-economic analysis.

ACKNOWLEDGEMENT

This work was supported by the Korea Institute of Energy Technology Evaluation and Planning (KETEP) and the Ministry of Trade, Industry & Energy (MOTIE) of the Republic of Korea (No. 20163030031790).

NOMENCLATURE

Abbreviations

CEPCI : chemical engineering plant cost index
COM : component object model
GT : gas turbine
MCFC : molten carbonate fuel cell
MGT : micro-gas turbine
ORC : organic Rankine cycle
PSO : particle swarm optimization
SOFC : solid oxide fuel
TAC : total annualized cost

Parameters

c_1 : self-adjustment weight
c_2 : social-adjustment weight
i : number of iterations
j : number of particles
t_{depr} : capital depreciation time [year]
t_{oper} : annual operating hours [h/year]
CI_n : chemical engineering plant cost index of year n
P_c : critical pressure [bar]
P_{elec} : electricity sales price [USD/kWh]
ΔP_{cond} : pressure drop of the condenser [bar]
T_c : critical temperature [°C]
Q_{IN} : heat transferred into the system [kW]

Variables

ψ_{ORC} : exergy efficiency of ORC
gbest : best solution found by the entire swarm
m_n : mass flow rate of steam n [kg/h]
pbest : best solution found by the particle
r_1, r_2 : random numbers uniformly distributed between [0, 1]
v : velocity vector
vf_n : vapor fraction of stream n
w : inertia weight of PSO algorithm
x : particle position
A : heat exchanger area [m^2]
$J_{capital}$: annualized capital cost [USD/year]
$J_{operation}$: annualized operation cost [USD/year]
P_n^{sat} : saturation pressure of stream n [bar]
PC_q : purchase and installation cost of equipment q [USD]
T_{AMB} : ambient temperature [°C]
T_{evap} : evaporation temperature [°C]
T_n : temperature of stream n [°C]
V_{cw} : volumetric flow rate of cooling water [m^3/h]
W_p : electricity consumed by equipment p
W_t : electricity generated from turbine [kW]

REFERENCES

1. K. Sugiura and I. Naruse, *J. Power Sources*, **106**, 51 (2002).
2. R. Bove, A. Moreno and S. McPhail, International status of molten carbonate fuel cell (MCFC) technology, JRC Scientific and Technical Reports (2008).
3. S. J. McPhail, L. Leto, M. D. Pietra and V. Moreno, International status of molten carbonate fuel cells technology, ENEA (2015).
4. T. Yamamoto, T. Furuhata, N. Arai and K. Mori, *Energy*, **26**, 239 (2001).
5. N. B. Desai and S. Bandyopadhyay, *Energy*, **34**, 1674 (2009).
6. A. V. Akkaya and B. Sahin, *Int. J. Energy Res.*, **33**, 553 (2008).
7. G. Angelino and P. C. di Paliano, *Energy Conversion Engineering Conference and Exhibit*, **2**, 1400 (2000).
8. S.-W. Ji, S.-K. Park and T.-S. Kim, *Transactions of the Korean Society of Mechanical Engineers B*, **34**, 907 (2010).
9. A. H. Mamaghani, B. Najafi, A. Shirazi and F. Rinaldi, *Energy*, **82**, 650 (2015).
10. M. Ebrahimi and I. Moradpoor, *Energy Convers. Manage.*, **116**, 120 (2016).
11. E. H. Wang, H. G. Zhang, B. Y. Fan, M. G. Ouyang, Y. Zhao and Q. H. Mu, *Energy*, **36**, 3406 (2011).
12. D. Sánchez, J. M. Muñoz de Escalona, B. Monje, R. Chacartegui and T. Sánchez, *J. Power Sources*, **196**, 4355 (2011).
13. A. Desideri, S. Gusev, M. van den Broek, V. Lemort and S. Quoilin, *Energy*, **97**, 460 (2016).
14. Z. Sun, S. Wang, F. Xu and W. He, *Energy Procedia*, **142**, 1222 (2017).
15. U. Lee and C. Han, *Comput. Chem. Eng.*, **83**, 21 (2015).
16. W. Li, X. Feng, L. J. Yu and J. Xu, *Appl. Therm. Eng.*, **31**, 4014 (2011).
17. J. Sarkar, *Energy*, **143**, 141 (2018).
18. E. Wang, H. Zhang, B. Fan and Y. Wu, *J. Mech. Sci. Technol.*, **26**, 2301 (2012).
19. M. Wang, R. Khalilpour and A. Abbas, *Energy Convers. Manage.*, **88**, 947 (2014).
20. S. Quoilin, M. Van Den Broek, S. Declaye, P. Dewallef and V. Lemort, *Renew. Sustain. Energy Rev.*, **22**, 168 (2013).
21. B. Patel, N. B. Desai, S. S. Kachhwaha, V. Jain and N. Hadia, *J. Clean. Prod.*, **154**, 26 (2017).
22. M. Asim, M. K. H. Leung, Z. Shan, Y. Li, D. Y. C. Leung and M. Ni, *Energy Procedia*, **143**, 192 (2017).
23. G. Xu and G. Yu, *J. Comput. Appl. Math.*, **333**, 65 (2018).
24. Y. Chen, L. Li, J. Xiao, Y. Yang, J. Liang and T. Li, *Eng. Appl. Artif. Intell.*, **70**, 159 (2018).
25. D. Tian and Z. Shi, *Swarm Evol. Comput.*, **41**, 49 (2018).
26. Z. L. Gaing, *IEEE Trans. Energy Convers.*, **19**, 384 (2004).
27. K. Park, W. Won and D. Shin, *J. Nat. Gas. Sci. Eng.*, **34**, 958 (2016).
28. A. Godio and A. Santilano, *J. Appl. Geophysics*, **148**, 163 (2018).
29. FuelCell Energy Solutions, http://www.all-energy.co.uk/__novadocuments/80806?v=635633926036100000 (accessed April 13, 2018).
30. S. Aghahosseini and I. Dincer, *Appl. Therm. Eng.*, **54**, 35 (2013).
31. N. Razaaly, G. Persico and P. M. Congedo, *Energy Procedia*, **129**, 1149 (2017).

32. S. Kwon, W. Won and J. Kim, *Renewable Energy*, **97**, 177 (2016).
33. S. Han, W. Won and J. Kim, *Energy*, **129**, 86 (2017).
34. W. Won, H. Kwon, J. Han and J. Kim, *Renewable Energy*, **103**, 226 (2017).
35. M. Kim, W. Won and J. Kim, *Energy Convers. Manage.*, **143**, 227 (2017).
36. H. P. Loh, J. Lyons and C. W. White III, Process equipment cost estimation, DOE/NETL-2002/1169 (2002).
37. W. Won and C. T. Maravelias, *Renewable Energy*, **114**, 357 (2017).
38. A. I. Papadopoulos and P. Seferlis, Materials and process systems for CO_2 capture: modeling, design, control, and integration, Wiley, New Jersey (2017).
39. EIA - Electricity Data https://www.eia.gov/electricity/monthly/epm_table_grapher.php?t=epmt_5_6_a (accessed March 3, 2018).
40. W10_TH_ Price Forecasts for Electric Motor CNG Compressor at Gas Station Project – EMERALD AACE 2017 – WEEKLY BLOG https://emeraldaace2017.com/2017/11/11/w10_th_-price-forecasts-for-electric-motor-cng-compressor-at-gas-station-project/ (accessed March 2, 2018).